OPEN ACCESS
JOURNAL OF ADVANCED DIELECTRICS
Vol. 13, No. 1 (2023) 2242002 (9 pages)

DOI: 10.1142/S2010135X22420024

Enhancement of permittivity and energy storage efficiency of poly (vinylidene fluoride-chlorotrifluoroethylene) by uniaxial stretching

Zhenji Zhou[*,†], Weimin Xia[†,‡,¶], Jing Liu[*], Na Tian[*] and Caiyin You[*,§,¶]

[*]*School of Materials Science and Engineering, Xi'an University of Technology Xi'an 710048, Shaanxi, P. R. China*

[†]*Faculty of Printing, Packaging, and Digital Media Technology Xi'an University of Technology, Xi'an 710048, Shaanxi, P. R. China*

[‡]xiaweimin@xaut.edu.cn

[§]caiyinyou@xaut.edu.cn

Received 1 June 2022; Revised 6 July 2022; Accepted 27 July 2022; Published 19 August 2022

Dielectric polymer film capacitors with a high-power density as well as efficient charge and discharge rates have great potential for application to fulfill the miniaturized and lightweight requirements of the electronic and stationary power systems. It was reported that the elastic recovery rate and energy storage density of poly (vinylidene fluoride-chlorotrifluoroethylene) [P(VDF-CTFE)] polymer film can be enhanced through thermostatic uniaxial stretching. But it is unknown about the relationship between the stretching rate and above properties. In this study, we investigated the effect of different stretching rates on the conformation, elastic recovery, dielectric constant, and energy storage density of stretched P(VDF-CTFE) polymer films. It was found that the stretching rate significantly affected the formation of polar β-crystal phase, causing different dielectric properties. The degrees of elastic recovery of P(VDF-CTFE) film vary with stretching rates. Among them, the elastic recovery rate of the P(VDF-CTFE) 94/6 film is 46.5% at a stretching rate of 15 mm/min, the dielectric constant is 12.25 at 100 Hz, and the energy density reaches 3.95 J/cm^3 with the energy loss of 39% at 200 MV/m field.

Keywords: P(VDF-CTFE); elastic recovery rate; energy density; dielectric properties.

1. Introduction

Polymer film capacitors are considered to be important electrical storage components for high-energy density pulse discharge capacitors due to their superior breakdown characteristics, charge–discharge rate (μs), and easy processing properties.[1–3] It significantly reduces the volume, weight, and cost of energy storage systems[4–7] and is widely used in flexible energy transmission systems, pulsed power supplies, electric vehicles, and electromagnetic energy equipment.[8,9] However, the low-energy density of polymer film capacitors is a key issue that limits commercial applications in high-energy density storage fields. Therefore, it is necessary to develop an effective method to further increase the dielectric constant and energy density of the polymers, which will contribute to the development of high-electric performance film capacitors.

For a linear dielectric material, the released energy density (U_e) of dielectric material can be expressed as an equation:

$$U_e = \frac{1}{2}\varepsilon_r\varepsilon_0 E_b^2, \tag{1}$$

where ε_0 is the vacuum dielectric constant ($\varepsilon_0 = 8.854 \times 10^{-12}$ F/m), ε_r is the material's relative permittivity and E_b is the dielectric breakdown strength.[10] Based on Eq. (1), the U_e of a polymer film is determined by the ε_r and E_b.[11–13] The dielectric constant of polymer nanocomposites can be increased by adding high-dielectric fillers, such as ferroelectric ceramics, and conductive particles (metal particles, graphite, and carbon nanotubes).[14–23] Usually, the concentration of high-dielectric filler is higher than 50 vol%, which leads to a decrease of E_b for the polymer nanocomposite due to a continuous conductive path. Thus, U_e of the polymer nanocomposite is depressed.[24] If the material is nonlinear or hysteretic, U_e of a capacitor in an external electric field can only be got by calculating the integral area between the discharging branch and the dielectric displacement axis of a dielectric displacement–electric field hysteresis loop, which is expressed as

$$U_e = \int_{D_r}^{D_{\max}} \vec{E}(\vec{D}) \cdot d\vec{D} \tag{2}$$

with the dielectric displacement given by the polarization $\vec{P}$ of the material and the ε_r of free space.

$$\vec{D} = \varepsilon_0 \cdot \vec{E} + \vec{P}(\vec{E}), \tag{3}$$

where E is the electric field, D_r and $D_{\max}$ are the electric displacement at zero field and the highest field, respectively.[25]

¶Corresponding authors.

It can be seen from Eq. (2) that the density is defined by the area between the discharge part of the *D–E* hysteresis loop and the dielectric displacement axis. Therefore, relaxor ferroelectric materials with high polarizability and slender hysteresis loops are more suitable for energy storage applications. At present, polymers exhibiting high polarizability, such as polypropylene (BOPP), polycarbonate (PC), polyethylene terephthalate (PET),[26] are promising to achieve a high-energy density. In addition, ferroelectric polyvinylidene fluoride (PVDF) and its copolymers, with trifluoroethylene (TrFE), hexafluoropropylene (HFP), chlorofluoroethylene (CFE), poly(methyl methacrylate) (PMMA), and chlorotrifluoroethylene (CTFE),[25,27–31] are also widely investigated by copolymerization,[32,33] grafting,[34,35] and cross-linking.[36–38]

Poly (vinylidene fluoride-chlorotrifluoroethylene) [P(VDF-CTFE)] is a binary copolymer composed of VDF and CTFE units with a certain ratio. The introduction of CTFE increases the disordering of the polymer molecular chain, thus making it easier for the dipole reorientation under an external electric field. When the content of CTFE is higher than 16.6 mol%,[39] the binary copolymer appears as an amorphous phase. In the case of low contents of VDF, the composite behaves as a semi-crystalline polymer with a hexagonal phase crystalline structure,[40] showing good dielectric properties owing to the strong polarity of C-F.[41] P(VDF-CTFE) copolymers were reported to show a relatively slim *D–E* loop under a high electric field.[42–44] A few research works have revealed that a low-temperature quenching or modifying the fillers of the composites could improve U_e of the P(VDF-CTFE) polymer.[33,45] Few studies have investigated how the stretch rate affects the elastic recovery, dielectric, and energy storage performance of pure P (VDF-CTFE) at high E_b.

In this work, the solution-casting was used to prepare the P(VDF-CTFE) films with different CTFE content. The stretching process is processed to prepare oriented P(VDF-CTFE) films by different stretching rates. P(VDF-CTFE) 94/6 presents high-dielectric properties and high-energy density. The maximum dielectric constant of the P (VDF-CTFE) 94/6 film reaches 12.25 at 100 Hz with a dielectric loss of 0.02 with a stretching rate of 15 mm/min. The energy density of the film was enhanced from 1.85 J/cm to 3.95 J/cm^3 at 200 MV/m, compared with the unstretched P(VDF-CTFE) film.

2. Experimental Section

2.1. *Materials*

P(VDF-CTFE) powders were purchased from Zhong Hao Chen Guang Chemical Research Institute, and the molar content of CTFE units was 6%, 9%, and 12%, respectively. N, N-dimethylformamide (DMF) solvent was bought from Wuxi Haisuo Biological Co. All the materials and solvents were used directly without further purification.

2.2. *Fabrication of P(VDF-CTFE) films*

Figure 1 presents a schematic of the preparation of P(VDF-CTFE) films, in which the structural formula and the molecular chain arrangement after stretching are also shown in the inset. The P(VDF-CTFE) powders were dissolved in DMF solution (the concentration of the solution was set to 15 g/mL) by continuously stirring at room temperature for 8 h. All P(VDF-CTFE) films were prepared by casting the copolymer solution onto a glass substrate. The coating was dried at 70°C for 6 h, followed by annealing under vacuum at 130°C for 4 h and slowly cooling down to room temperature. Finally, the films were soaked in distilled water to peel them off. The prepared films are denoted as A, B, and C, corresponding to the molar content of CTFE of 12%, 9%, and 6%, respectively. Then, the solution-casting films were uniaxially stretched under air circulation at 50°C. The stretched film is marked as C*n*, where *n* represents the stretching rate (*n* mm/min). The stretched film was further annealed under tension at 50°C for 15 min to release internal stresses. The center view of Fig. 1 is the scheme of molecular chain orientation of the P(VDF-CTFE) film before and after uniaxial stretching. The final thickness of free-standing films is around 15 μm.

2.3. *Characterizations*

Au electrodes were deposited onto the films using an ion sputter coater (IXRF MSP-2S, Japan), with a diameter of 3 mm. X-ray diffraction (XRD-700, SHIMADZU, Japan), Differential scanning calorimeter (DSC, Netzsch, TA-Q2000, Germany) were utilized to characterize the phase components of the films. Fourier transform infrared spectroscopy (FTIR, IRspirit, Hitachi, Japan) was used to characterize the crystalline structure and chain conformation of the samples. The electronic universal testing machine (UTN7104H, Shen Zhen san si, China) was used to stretch the P(VDF-CTFE) films. The dielectric property was characterized at different frequencies (10^2–10^7Hz) using Novocontrol Concept 40.

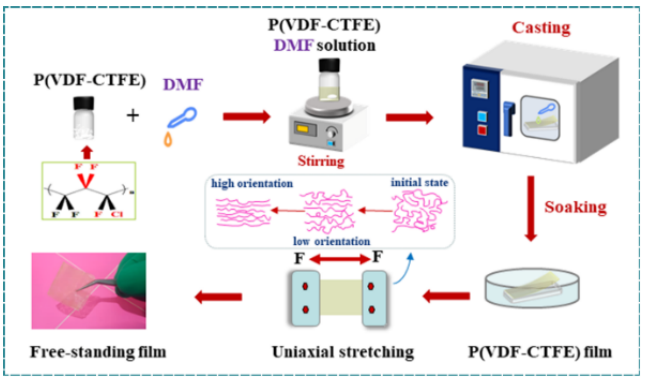

Fig. 1. Schematic illustration of the preparation of P(VDF-CTFE) film and the scheme of molecular chain orientation in the film before and after uniaxial stretching.

The electric displacement–electric field loops (D–E loops) were obtained by a TF Analyzer 2000 ferroelectric test system under the electric field with a triangular waveform at a frequency of 10 Hz. The values of elastic recovery (E_r) were obtained by taking the average of the four measurements.

3. Results and Discussion

3.1. *Mechanical properties of P(VDF-CTFE) films*

The elastic recovery rate (E_r) of the P(VDF-CTFE) film is tested by the universal material testing machine. Here, the P(VDF-CTFE) film with a length of 30 mm was stretched to 400% deformation at different stretching rates and maintained for 15 min. Then, the stress load was removed and the sample was left in a relaxed state for 30 min. Finally, the straightened length of the sample is measured as reversion length. The E_r is calculated as follows[46]

$$E_r = \frac{L_1 - L_2}{L_1 - L_0} * 100\%, \tag{4}$$

where L_1 is the total length of the film after stretching, L_2 is the length of the film after reversion and L_0 is the original length of the sample film before stretching (original scale). Figure 2(a) shows that the elastic recovery rate of the P(VDF-CTFE) film decreases with the content of the CTFE at the same stretching rate. The films were stretched at varied rates of 5, 10, 15, and 20 mm/min to study the effect of the stretching rate on the elastic recovery rate of P(VDF-CTFE) films. It was found that the elastic recovery rate of the P(VDF-CTFE) films increased with increasing stretching rate. When the stretching rate is 20 mm/min, the elastic recovery rate reaches 55%. Figure 2(b) shows the stress–strain curves of P(VDF-CTFE) films. The stress–strain curves of all films have typical yield points. After the yield point, the stresses of the films show a tendency of first decrease and then slowly increase. The large deformation of the material after the yield point is mainly due to the movement of the originally frozen chain segments. In addition, the film necking happens during the uniaxial stretching process, causing the phase transition from a spherulitic structure to a fine fibrous structure. It was considered that there exists a transition from α phase to β phase under the necking process.[47,48] Figures 2(c) and 2(d) show SEM images of P(VDF-CTFE) 94/6% before and after stretching (15 mm/min), respectively. It can be seen that the morphology of the P(VDF-CTFE) film changed after stretching along the direction of the external force, indicating that the stretching caused a deformation of the film.

3.2. *Crystalline properties*

Figure 3(a) shows the XRD patterns of the P(VDF-CTFE) films. Regarding PVDF-based polymers, the diffraction peaks at 2θ = 17.66°, 19.2°, and 20.4° correspond to α phase (100), γ phase (020), and β phase (110/200), respectively.[49,50] So, the films with different CTFE contents present the mixed phases of α, β, and γ before stretching. After stretching, the overlapping peaks at 2θ = 17.66°, 19.2° become weak or even disappear. The diffraction peak of the β phase at 2θ = 20.4° becomes strong, indicating that the stretch process is

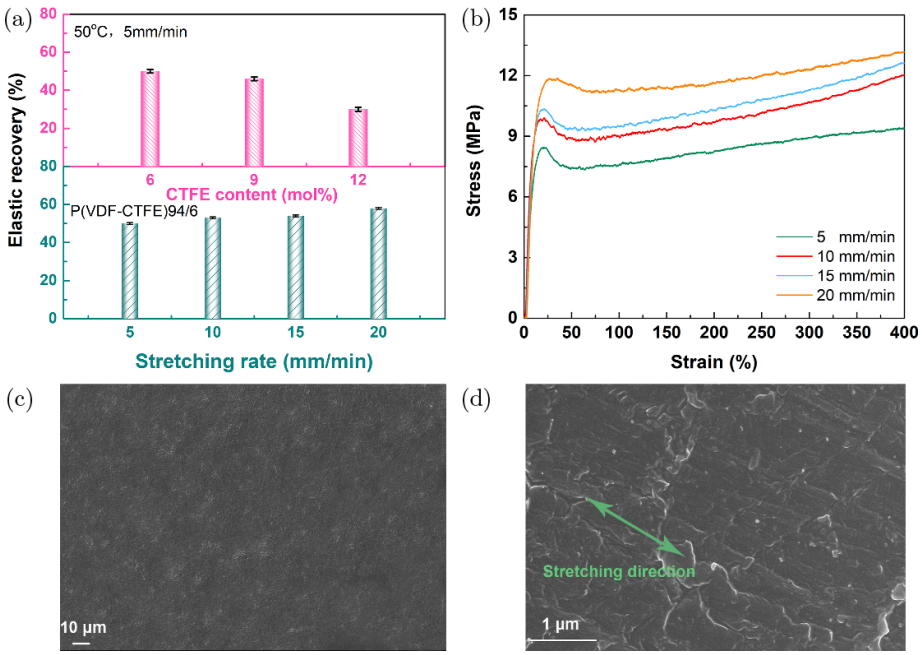

Fig. 2. (a) Influence of CTFE content and stretching rate on P(VDF-CTFE) casting films' elastic recoveries; (b) the stress–strain curves of P(VDF-CTFE) 94/6 film. SEM images of P(VDF-CTFE) 94/6 mol% film (c) before and (d) after being uniaxially stretched (5 mm/min).

helpful for the phase transition from α to β. This is because the stretching promotes the rearrangement of the molecular chains along the direction of stress, leading to a transition from α to β phase and an increase in dipole density. At the same time, the denseness of the film and the ordering of the crystals are also improved. Figure 3(b) gives the DSC curves of the P(VDF-CTFE) films before and after stretching. All films show two peaks, corresponding to Curie temperature (T_c) and melting temperature (T_m). T_m of P(VDF-CTFE) decreases from 130°C to 84.2°C as the CTFE content decreased from 12% to 6%. T_m (127.6°C) of the stretched film is a little lower than the value of the unstretched film (130.8°C) and the endothermic peak becomes wide.

Figure 4 shows the typical FTIR spectra of P(VDF-CTFE) 94/6 mol% films with different stretching rates. The polymer chains have obvious bands at 1279, 1234, 840, 764 and 512 cm^{-1}, indicating that crystalline α, β, and γ phases coexist in the stretched P(VDF-CTFE) film.[51,52] As the stretching rate increases, the intensity of the absorption peak at 840 cm^{-1} increases, indicating the transformation of the α phase to the β phase. The FTIR results are consistent with the XRD results shown in Fig. 3(a). The relative proportion of the β phase ($F(\beta)$) in the sample can be calculated based on the infrared spectrum given in the following equations[53]:

$$F_{\beta,\gamma} = \frac{A_{840}}{(K_{840}/K_{764})A_{\alpha 764} + A_{\beta 840}} \times 100\%, \quad (5)$$

$$F_{\alpha} = 100\% - F_{\beta,\gamma}, \quad (6)$$

$$F_{\beta} = F_{\beta,\gamma} \times \left(\frac{A_{\beta}}{A_{\beta} + A_{\gamma}}\right) \times 100\%, \quad (7)$$

where A_β and A_γ are the integrated areas of β and γ phases based on the deconvolution curves of FTIR peaks at 840 cm^{-1}. A_{764} and A_{840} are the absorption peak intensities at 764 cm^{-1}, 840 cm^{-1}, respectively; 6.1 × 10^4 cm^2/mol of K_α and 7.7 × 10^4 cm^2/mol of K_β are the absorption coefficients of α and β phases. $F(\beta)$ is the total relative proportion of electroactive β. The calculated results are listed in Fig. 4(b). It can be found that the portions of polar crystal phases increase with the stretching rate. Furthermore, the $F(\beta)$ of 58.5% for C15

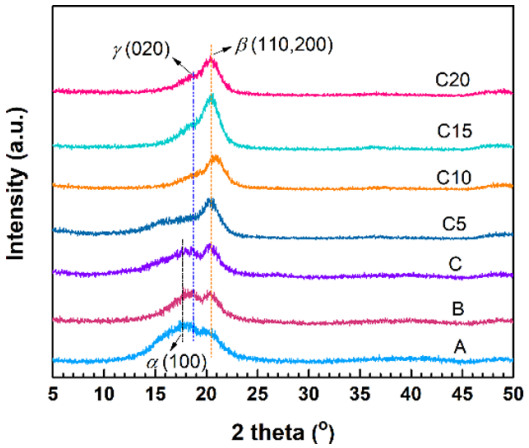

(a)

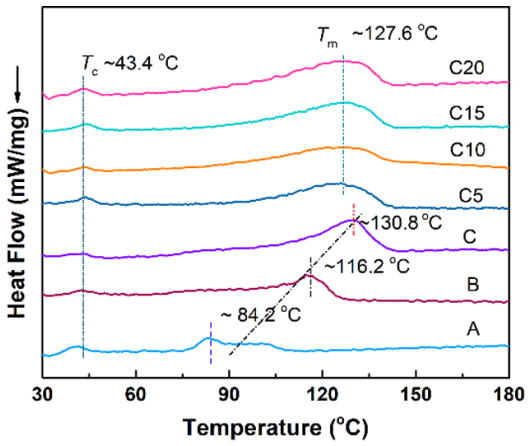

(b)

Fig. 3. (a) XRD patterns, (b) DSC curves of P(VDF-CTFE) films with different amounts of CTFE and at different stretching rates.

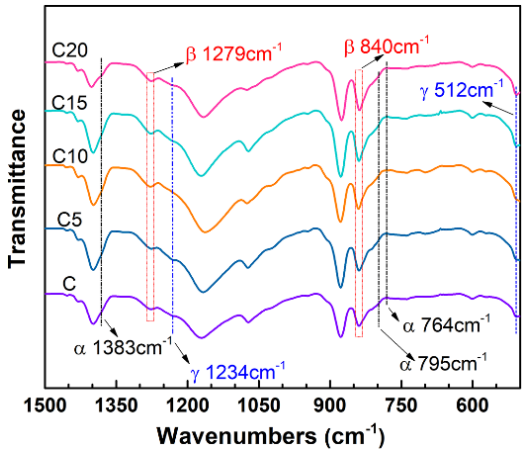

(a)

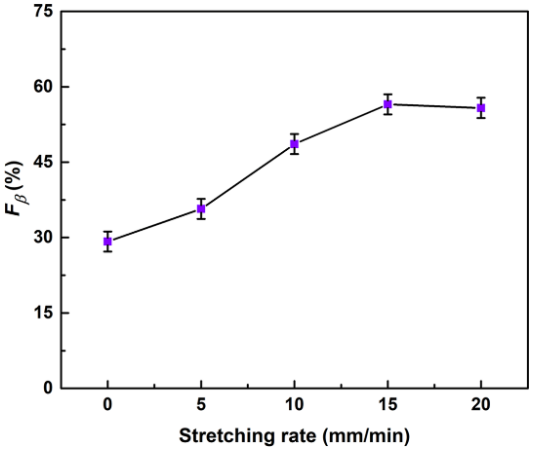

(b)

Fig. 4. (a) FTIR spectra of P(VDF-CTFE) films at different stretching rates, (b) the relative β-phase fractions.

can be achieved when the stretching rate is 15 mm/min. It can be considered that during the stretching process, the α crystal form will be highly oriented and arranged due to the uniform external force, resulting in a change from a cis conformation to an all-trans conformation, increasing the β phase.

3.3 *Dielectric property and breakdown behaviors of P(VDF-CTFE) films*

Figure 5 gives the relative permittivity (ε_r), dielectric loss (tanδ) of P(VDF-CTFE) films in the frequency range of 10^2 Hz to 10^7 Hz, and a Weber distribution to explore the effect of the stretching rate on breakdown strength. ε_r of the stretched P(VDF-CTFE) film is higher than that of the unstretched sample and increases with the stretching rate due to the enhanced ordering of the molecular chains.[54,55] When the frequency of the external electric field is higher than the relaxation frequency (100 kHz) of the dipole, ε_r decreases with further increasing frequency. At a high frequency, the dipole moment and segment motion cannot keep up with the change of electric field frequency. At frequencies above 10^4 Hz, dipole relaxation leads to a rapid increase of tanδ. The dielectric loss of the unstretched sample is about 0.12 at 10^2 Hz, while the stretched sample was lower than 0.05 at the same frequency, which can be explained by the restricted mobility of the polymer chains. The molecular chains and segments of the molecular chain are unwrapped by an external force during stretching, which could also increase the free volume. On the other hand, the dielectric constant and loss present a slight change with further increasing stretching rate. It can be deduced that the film compacting was also accompanied with the potential disruption of the molecular chain. Thus, the dielectric properties could not be further enhanced through increasing the stretching rate.

The breakdown strength is a critical metric of dielectric materials. The breakdown strength of C, C5, C10, C15, and C20 film was tested, and the results were analyzed using Weibull distribution function[56]

$$P(E) = 1 - \exp\left[-\left(E/E_b\right)^{\beta}\right],$$

where $P(E)$ is the cumulative probability of voltage breakdown, E is the measured breakdown field, E_b is the breakdown strength when the cumulative breakdown probability is 63.2%, and β is the slope parameter of Weibull fitting curve. The fitting results are shown in Fig. 5(c); β equals 17.3, 26.9, 28.6, 31.8, and 22.8. The Weibull breakdown strengths of P(VDF-CTFE) films are 200.1, 205.5, 207.4, 211.6, and 209.3 MV/m, respectively (Fig. 5(d)). As the stretching rate increased, the breakdown electric field also increased. The breakdown field of P(VDF-CTFE) films decreases when the stretching rate is 20 mm/min. This is because the rapid

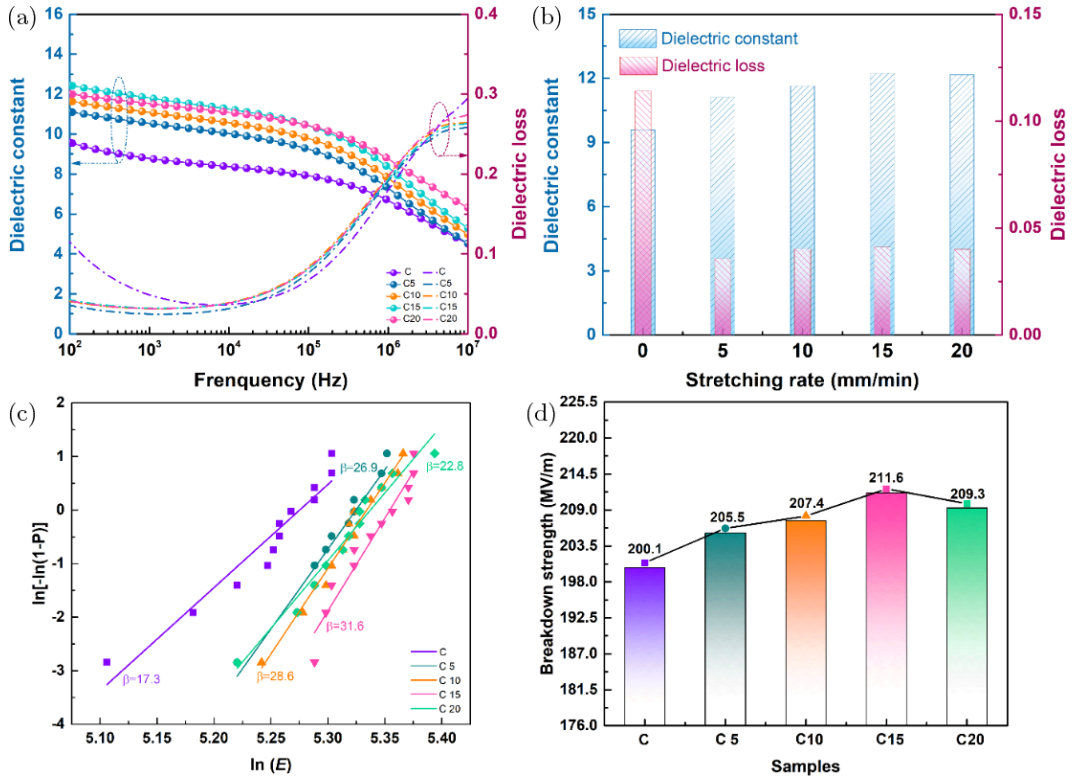

Fig. 5. (a) The dielectric permittivity and dielectric loss versus frequency of five P(VDF-CTFE) 94/6 mol% films at 100 Hz. (b) The dielectric constant and dielectric loss of five P(VDF-CTFE) 94/6 mol% films at 100 Hz. (c) The Weibull analysis of breakdown strength of five P(VDF-CTFE) 94/6 mol% films. (d) Weibull breakdown strength of five P(VDF-CTFE) 94/6 mol% films.

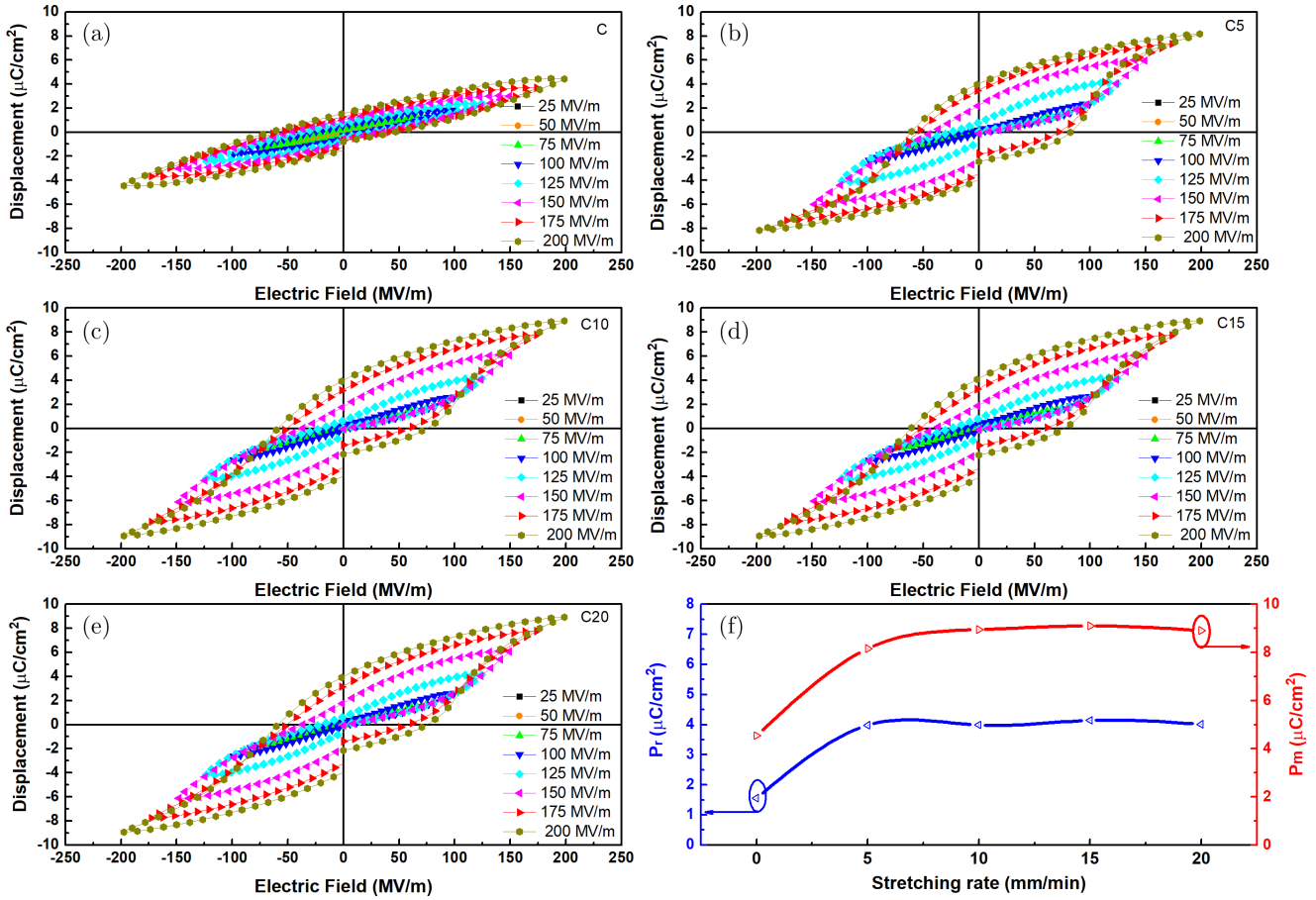

Fig. 6. Bipolar *D–E* loops for P(VDF-CTFE) films at room temperature (a) C sample, (b) C5 sample, (c) C10 sample, (d) C15 sample, (e) C20 sample, and (f) relationship between stretching rate and P_r and P_m at 200 MV/m. The tests were performed at room temperature, and the poling frequency was 10 Hz with a sinusoidal waveform.

stretching rate could result in local stresses and some structural defects, thus reducing the breakdown strength of the polymer film.

Figure 6 shows the bipolar *D–E* loops of P(VDF-CTFE) 94/6 mol% films and a comparison of P_r with P_m under an applied electric field of 200 MV/m. All measurements were performed at a frequency of 10 Hz with an electric field of 25 MV/m increment. As shown in Fig. 6(a), the *D–E* loop of unstretched P(VDF-CTFE) film shows a spindly loop under a high electric field of 200 MV/m, indicating a feature of linear dielectric with some leakage. However, the stretched P(VDF-CTFE) films show a different polarizing process, as shown in Figs. 6(b)–6(e). The electric hysteresis loops are linear-shaped in the case of the applied external electric field being less than 75 MV/m. When the electric field is lower than the coercive electric field, the electric displacement mainly comes from the vibration of the molecular chain, electrons, and atomic polarization.[57] As the electric field continues to increase, dipole polarization plays a dominant role. Even when the electric field reaches 200 MV/m, the *D–E* loops of the stretched P(VDF-CTFE) films cannot reach saturation. Figure 6(f) shows the dependences of remanent polarization (P_r) and maximum polarization (P_m) on the stretching rate. The electric displacement value remained stable when the stretching rate was greater than 15 mm/min. The sample of C15 gets the largest P_m and P_r values of 9.12 μC/cm^2 and 4.14 μC/cm^2, respectively.

3.4. *Energy storage properties of P(VDF-CTFE) films*

Figure 7(a) gives the unipolar *D–E* hysteresis loops under 175 MV/m to further evaluate the effect of CTFE content on the energy storage performance of ferroelectric polymers. Both P_r and P_m of C samples remained at low values compared to A and B samples. In addition, the P_r of the C sample was 3.02 μC/cm^2, while P_m of the film after stretching was 7.25 μC/cm^2 under the electric field of 175 MV/m as shown in Fig. 7(b). Figure 7(c) gives the unipolar *D–E* loops of four stretched P(VDF-CTFE) films at 200 MV/m. Figure 7(d) shows the charging energy density and loss as a function of the stretching rate. U_{charged} of the stretched films has a larger value. U_{charged} values of C5–C20 are 3.34, 3.73,

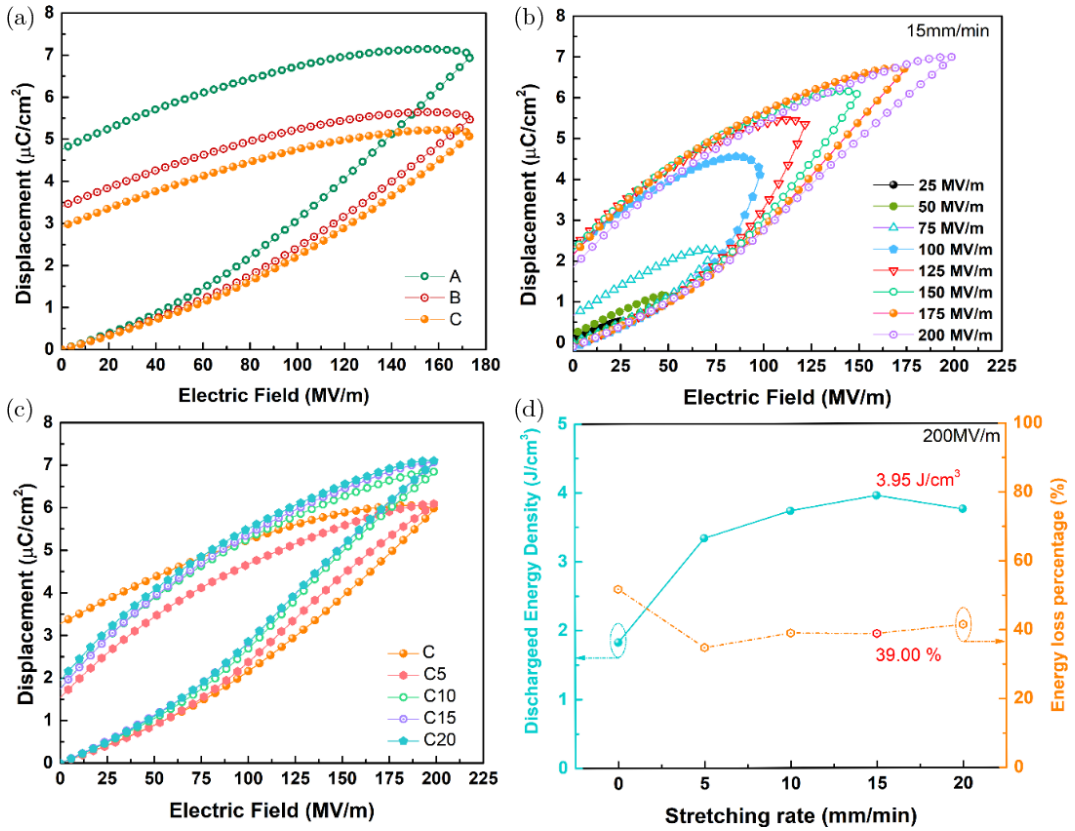

Fig. 7. Unipolar *D–E* loops of (a) un-stretching P(VDF-CTFE) films with different CTFE content, (b) stretched C sample at various electric fields, (c) stretched C sample films at different stretching rates, and (d) energy storage density and percentage energy loss of C sample films as a function of stretching rate.

3.95, and 3.75, respectively, which are greater than 1.83 of C sample. The energy loss of C15 sample is the smallest, only 39%. So, a large energy density was achieved simultaneously with a high-dielectric constant and low-dielectric loss under a proper stretching rate.

4. Conclusions

This work demonstrates that the stretching can enhance the dielectric property and energy storage capability of P(VDF-CTFE) films. It was found that the isothermal uniaxial stretching of the P(VDF-CTFE) polymer film further induced the transformation of P(VDF-CTFE) crystals from α phase to β phase, which reduces the formation of internal defects and improved the denseness of the polymer film. The dielectric constant in C15 was 12.2 at 100 Hz with a dielectric loss of 0.03 due to the improved ordering of the molecular chains after stretching. This method effectively increases the dielectric constant of the material while reducing the dielectric loss of the polymer film. The energy density of C15 film achieves 3.95 J/cm^3 with an energy loss of 39% at 200 MV/m. A promising P(VDF-CTFE) film was proposed as a candidate with high-energy density for flexible film capacitor.

Acknowledgment

This work is in part supported by ISF-SFC joint research program (No. 51961145305), Key Research and Development Program of Shaanxi Province (No. 2021KWZ-12), Doctoral Dissertation Innovation Fund of Xi'an University of Technology (No. 252072103), and the Youth Innovation Team of Shaanxi Universities contributed equally to this work.

References

[1]Y. Tian, Q. Qian, Y. Sheng, X. Zhang, H. Wu and H. Ye, High-energy density in poly(vinylidene fluoride-trifluoroethylene) composite incorporated with modified halloysite nanotubular architecture, *Colloid Surf. A* **625**, 126993 (2021), https://doi:10.1016/j.colsurfa. 2021.126993.

[2]M. Li, H. Wondergem, M. J. Spijkman, K. Asadi, I. Katsouras, P. W. M. Blom and D. M. D. Leeuw, Revisiting the δ-phase of poly(vinylidene fluoride) for solution-processed ferroelectric thin films, *Nat. Mater.* **12**, 433438 (2013), https://doi:org/10.1038/nmat3577.

[3]B. Chu, X. Zhou, K. Ren, B. Neese, M. Lin, Q. Wang, F. Bauer and Q. M. Zhang, A dielectric polymer with high electric energy density and fast discharge speed, *Science* **313**, 334 (2006), https://doi:10.1126/science.1127798.

[4]Y. Yang, J. He, Q. Li, L. Gao, J. Hu, R. Zeng, J. Qin, X. S. Wang and Q. Wang, Self-healing of electrical damage in polymers using

superparamagnetic nanoparticles, *Nat. Nanotechnol.* **14**, 151 (2019), https://doi:10.1038/s41565-018-0327-4.

[5]C. Ribeiro, C. M. Costa, D. M. Correia, J. Nunes-Pereira, J. Oliveira, P. Martins, R. Goncalves, V. F. Cardoso and Lanceros-Mendez, Electroactive poly(vinylidenefluoride)-based structures for advanced applications, *Nat. Protoc.* **13**, 681 (2018), https://doi:10.1038/nprot.2017.157.

[6]Y. Hao, X. Wang, K. Bi, J. Zhang, Y. Huang, L. Wu, P. Zhao, K. Xu, M. Lei and L. Li, Ultrafine core-shell $BaTiO_3$@SiO_2structures for nanocomposite capacitors with high energy density, *Nano Energy* **31**, 49 (2017), https://doi:10.1016/j.nanoen.2018.07.006.

[7]H. Ye, Q. Wang, Q. Sun and L. Xu, High energy density and interfacial polarization in poly(vinylidene fluoride-chlorotrifluoroethylene) nanocomposite incorporated with halloysite nanotube architecture, *Colloid Surf. A* **606**, 125495 (2020), https://doi:10.1016/j.colsurfa.2020.125495.

[8]Z. M. Dang and M. Zheng, *Dielectric polymer materials for high-density energy storage*, 7 Multiphase/multicomponent dielectric polymer materials with high permittivity and high breakdown strength (William Andrew Publishing, 2018), pp. 247–287. https://doi:10.1016/B978-0-12-813215-9.00007-5.

[9]B. H. Guo, Dai, J. L. Han, Y. Gao, J. R. He, Z. H. Dai and J. Xu, Increased dielectric permittivity of poly(vinylidene-fluoride-co-chlorotrifluoroethylene) nanocomposites by coating $BaTiO_3$with functional groups owning high bond dipole moment, *Colloid Surf. A* **529**, 560 (2017), https://doi:10.1016/j.colsurfa.2017.05.065.

[10]W. S. Wang, Y. Jing and Z. C. Liu, Dielectric and energy storage properties of PVDF films with large area prepared by solution tape casting process, *IEEE Trans. Dielect. Electr. Insul.* **24**, 697 (2017), https://doi:10.1109/TDEI.2017.006148.

[11]N. Meng, X. Ren, G. Santagiuliana, L. Ventura, H. Zhang, J. Wu, H. Yan, M.J. Reece and E. Bilotti, Ultrahigh β-phase content poly(vinylidene fluoride) with relaxor-like ferroelectricity for high energy density capacitors, *Nat. Commun.* **10**, 4535 (2019), https://doi:10.1038/s41467-019-12391-3.

[12]R. P. Nie, Y. Li, L. C. Jia, J. Lei, H. D. Huang and Z. M. Li, PVDF/PMMA dielectric films with notably decreased dielectric loss and enhanced high-temperature tolerance, *J. Polym. Sci. Part B Polym Phys.* **57**, 1043 (2019), https://doi:10.1002/polb.24858.

[13]T. Zhang, X. Zhao, C. Zhang, Y. Zhang, Y. Zhang, Y. Feng, Q. Chi and Q. Chen, Polymer nanocomposites with excellent energy storage performances by utilizing the dielectric properties of inorganic fillers, *Chem. Eng. J.* **408**, 127314 (2021), https://doi:10.1016/j.cej.2020.127314.

[14]K. Wu, J. Wang, D. Liu, C. Lei, D. Liu, W. Lei and Q. Fu, Highly thermoconductive, thermostable, and super-flexible film by engineering 1D rigid rod-like aramid nanofiber/2D boron nitride nanosheets, *Adv. Mater.* **32**, 1906939 (2020), https://doi:10.1002/adma.201906939.

[15]Y. Zhu, H. Yao, P. Jiang, J. Wu, X. Zhu and X. Huang, Two-dimensional high-k nanosheets for dielectric polymer nanocomposites with ultrahigh discharged energy density, *J. Phys. Chem. C* **122**, 18282 (2018), https://doi:10.1021/acs.jpcc.8b04918.

[16]J. Wang, H. Chen, X. Li, C. Zhang, W. Yu, L. Zhou, Q. Yang, Z. Shi and C. Xiong, Flexible dielectric film with high energy density based on chitin/boron nitride nanosheets, *Chem. Eng. J.* **383**, 123147 (2020), https://doi:10.1016/j.cej.2019.123147.

[17]B. Zhang, X. M. Chen, W. W. Wu, A. Khesro, P. Liu, M. M. Mao, K. X. Song, R. Sun and D. W. Wang, Outstanding discharge energy density and efficiency of the bilayer nanocomposite films with BaTiO3-dispersed PVDF polymer and polyetherimide layer, *Chem. Eng. J.* **446**, 136926 (2022), https://doi.org/10.1016/j.cej.2022.136926.

[18]N. Tsutsumi, R. Kosugi, K. Kinashi and W. Sakai, Nature of the enhancement in ferroelectric properties by gold nanoparticles in vinylidene fluoride and trifluoroethylene copolymer, *ACS Appl. Mater. Interf.* **8**, 16816 (2016), https://doi:10.1021/acsami.6b05897.

[19]M. Yang, H. Zhao, D. He and J. Bai, Constructing a continuous amorphous carbon interlayer to enhance dielectric performance of carbon nanotubes/polyvinylidene fluoride nanocomposites, *Carbon* **116**, 94 (2017), https://doi:10.1016/j.carbon.2017.01.105.

[20]J. Chen, Y. Wang, X. Xu, Q. Yuan, Y. Niu, Q. Wang and H. Wang, Ultrahigh discharge efficiency and energy density achieved at low electric fields in sandwich-structured polymer films containing dielectric elastomers, *J. Mater. Chem. A* **7**, 3729 (2019), https://doi:10.1039/C8TA11790J.

[21]G. Wang, J. L. Li, X. Zhang, Z. M. Fan, F. Yang, A. Feteira, D. Zhou, D. C. Sinclair, T. Ma, X. L. Tan, D. W. Wang and I. M. Reaney, Ultrahigh energy storage density lead-free multilayers by controlled electrical homogeneity, *Energy Environ. Sci.* **12**, 582 (2019), https://doi.org/10.1039/C8EE03287D.

[22]L. Y. Wu, K. Wu, C. X. Lei, D. Y. Liu, R. N. Du, F. Chen and Q. Fu, Surface modifications of boron nitride nanosheets for poly(vinylidene fluoride) based film capacitors: Advantages of edge-hydroxylation, *J. Mater. Chem. A* **7**, 7664 (2019), https://doi:10.1039/C9TA00616H.

[23]B. Liu, M. Yang, W. Zhou, H. Cai, S. Zhong, M. Zheng and Z. Dang, High energy density and discharge efficiency polypropylene nanocomposites for potential high-power capacitor, *Energy Storage Mater.* **27**, 443 (2020), https://doi:10.1016/j.ensm.2019.12.006.

[24]H. Ye, X. Zhang, C. Xu and L. Xu, Few-layer boron nitride nanosheets exfoliated with assistance of fluoro hyperbranched copolymer for poly (vinylidene fluoride-trifluoroethylene) nanocomposite film capacitor, *Colloid Surf. A* **580**, 123735 (2019), https://doi:10.1016/j.colsurfa.2019.123735.

[25]Y. Hambal, V.V. Shvartsman, D. Lewin, C. H. Huat and D. C. Lupascu, Effect of composition on polarization hysteresis and energy storage ability of P(VDF-TrFE-CFE) relaxor terpolymers, *Polymers* **13**, 1343 (2021), https://doi:10.3390/polym13081343.

[26]J. M. Carr, M. Mackey, L. Flandin, D. Schuele, L. Zhu and E. Baer, Effect of biaxial orientation on dielectric and breakdown properties of poly (ethylene terephthalate)/poly (vinylidenefluoride-co-tetrafluoroethylene) multilayerfilms, *J. Poly. Sci. B Poly. Phys.* **51**, 882 (2013), https://doi:10.1002/polb.23277.

[27]L. Zhu, Exploring strategies for high dielectric constant and low loss polymer dielectrics, *J. Phys. Chem. Lett.* **5**, 3677 (2014), https://doi:10.1021/jz501831q.

[28]K. Kim, H. B. Jung, J. H. Lim, S. Y. Ji and D. Y. Jeong, Configurational approach to the enhancement of the dielectric properties and energy density of PVDF-based polymer composites, *J. Phys. D Appl. Phys.* **53**, 375502 (2020), https://doi:10.1088/1361-6463/ab88e4.

[29]C. Li, L. Shi, W. Yang, Y. Zhou, X. Li, C. Zhang and Y. Yang, All polymer dielectric films for achieving high energy density film capacitors by blending poly(vinylidene fluoride-trifluoroethylene-chlorofluoroethylene) with aromatic polythiourea, *Nanoscale Res. Lett.* **15**, 1 (2020), https://doi:10.1186/s11671-020-3270-x.

[30]D. Thuau, K. Kallitsis, S. Ha, F. Bargain, T. Soulestin, G. Pecastaings, S. Tencé-Girault, F. D. D. Santos and G. Hadziioannou, High and temperature-independent dielectric constant dielectrics from PVDF-based terpolymer and copolymer blends, *Adv. Electron. Mater.* **6**, 1901250 (2020), https://doi:10.1002/aelm.201901250.

[31]B. Chu and Y. Zhou, Energy storage properties of PVDF terpolymer/PMMA blends, *High Volt.* **1**, 171 (2016), doi:10.1049/hve.2016.0062.
[32]Z. Zhang and T. C. M. Chung, Study of VDF/TrFE/CTFE terpolymers for high pulsed capacitor with high energy density and low energy loss, *Macromolecules* **40**, 783 (2007), https://doi:10.1021/ma0627119.
[33]W. M. Xia, Z. Xu, F. Wen, W. Li and Z. C. Zhang, Crystalline properties dependence of dielectric and energy storage properties of poly (vinylidene fluoride-chlorotrifluoroethylene), *Appl. Phys. Lett.* **97**, 1133 (2010), https://doi:10.1063/1.3518921.
[34]F. Guan, J. Wang, L. Yang, J. K. Tseng, K. Han, Q. Wang and L. Zhu, Confinement-induced high-field antiferroelectric-like behavior in a Poly(vinylidene fluoride-co-trifluoroethylene-co-chlorotrifluoroethylene)-graft-polystyrene graft copolymer, *Macromolecules* **44**, 48 (2011), https://doi:10.1021/ma102910v.
[35]J. Li, S. Tan, S. Ding, H. Li, L. Yang and Z. Zhang, High-field antiferroelectric behaviour and minimized energy loss in poly (vinylidene-co-trifluoroethylene)-graft-poly (ethyl methacrylate) for energy storage application, *J. Mater. Chem. C* **22**, 23468 (2012), https://doi:10.1039/C2JM35532A.
[36]Y. Chen, X. Zhao and Q. Shen, Regulation of energy storage capacitance and efficiency in semi-crystalline vinylidene fluoride copolymers through cross-linking method, *IEEE Trans. Dielect. Electr. Insul.* **24**, 682 (2017), https://doi:10.1109/TDEI.2017.006276.
[37]X. Chen, Z. Li, Z. Cheng, J. Zhang, Q. Shen, H. Ge and H. Li, Greatly enhanced energy density and patterned films induced by photo cross-linking of poly (vinylidene fluoride-chlorotrifluoroethylene), *Macromol. Rapid Comm.* **32**, 94 (2011), https://doi:10.1002/marc.201000478.
[38]Y. Chen, X. Tang, J. Shu, X. Wang, W. Hu and Q. Shen, Cross-linked P(VDF-CTFE)/PS-COOH nanocomposites for high-energy-density capacitor application, *J. Polym. Sci. Part B: Polym. Phys.* **54**, 1160 (2016), https://doi:10.1002/polb.24023.
[39]N. K. Kalfoglou and H. L. Williams, Mechanical relaxations of poly(vinylidene fluoride) and some of its copolymers, *J. Appl. Polym. Sci.* **17**, 3367 (1973), https://doi:10.1002/app.1973.070171111.
[40]Z. Wang, Z. Zhang and T. Chung, High dielectric VDF/TrFE/CTFE terpolymers prepared by hydrogenation of VDF/CTFE copolymers: Synthesis and characterization, *Macromolecules* **3**, 4268 (2006), doi:10.1021/ma060738m.
[41]A. J. Lovinger, Ferroelectric polymers, *Science* **220**, 1115 (1983), https://doi:10.1126/science.220.4602.1115.
[42]X. Lu, Y. Tang and Z. Y. Cheng, Fabrication and characterization of free-standing, flexible and translucent $BaTiO_3$-P(VDF-CTFE) nanocomposite films, *J. Alloys Compd.* **770**, 327 (2018), https://doi:10.1016/j.jallcom.2018.08.185.
[43]X. Lu, L. Zhang, Y. Tong and Z. Y. Cheng, BST-P(VDF-CTFE) nanocomposite films with high dielectric constant, low dielectric loss, and high energy-storage density, *Compos. Part B: Eng.* **168**, 34 (2019), https://doi:10.1016/j.compositesb.2018.12.059.
[44]Z. Li, Y. Wang and Z. Y. Cheng, Electromechanical properties of poly (vinylidenefluoride-chlorotrifluoroethylene) copolymer, *Appl. Phys. Lett.* **88**, 062904 (2006), https://doi:10.1063/1.2170425.
[45]Y. Li, J. Xiao, L. Li, J. Ye, F Wen, P. Dong, Y. Xie, J. Ding and Y. Zhang, Blends based P(VDF-CTFE) with quenching in ice water and PLZST modification with high energy storage performance, *Polymer* **202**, 122727 (2020), https://doi:10.1016/j.polymer.2020.122727.
[46]Y. Xu, W. Wang, Z. Liu, T. Rong, Q. Yu, P. Deng and Y. Pan, Preparation and characterization of poly (vinylidene fluoride) hard elastic membrane, *ShanDong Chem. Indus*. **48**, 62 (2019), https://doi:10.19319/j.cnki.issn.1008-021x.2019.15.025.
[47]M. Yoo, C. W. Frank, S. Mori and S. Yamaguchi, Effect of poly (vinylidene fluoride) binder crystallinity and graphite structure on the mechanical strength of the composite anode in a lithium-ion battery, *Polymer* **44**, 4197 (2003), https://doi:10.1016/S0032-3861(03)00364-1.
[48]B. Mohammadi, A. A. Yousefi and S. M. Bellah, Effect of tensile strain rate and elongation on crystalline structure and piezoelectric properties of PVDF thin films, *Polym. Test.* **26**, 42 (2007), https://doi:10.1016/j.polymertesting.2006.08.003.
[49]W. M. Xia, F. Liang, J. H. Xing and Z. Xu, Dielectric property, electric breakdown, and discharged energy density of a poly-(vinylidene fluoride-co-chlorotrifluoroethylene) copolymer with low temperature processing, *J. Appl. Polym. Sci.* **132**, 42794 (2015), https://doi:10.1002/app.42794.
[50]X. Wang, B. B. Qiao, S. B. Tan, W. Zhu and Z. C. Zhang, Tuning ferroelectric phase transition of PVDF by uniaxially stretching crosslinked PVDF films with CF=CH bonds, *J. Mater. Chem. C* **8**, 11426 (2020), https://doi:10.1039/D0TC02559C.
[51]R. G. Jr and R. C. Capitao, Morphology and phase transition of high melt temperature crystallized poly (vinylidene fluoride), *J. Mater. Sci.* **35**, 299 (2000), https://doi:10.1023/A:1004737000016.
[52]P. Martins, A. C. Lopes and S. Lanceros-Mendez, Electroactive phases of poly (vinylidene fluoride): Determination, processing and applications, *Prog. Polym. Sci.* **39**, 683 (2014), https://doi:10.1016/j.progpolymsci.2013.07.006.
[53]B. Lin, L. H. Pan, D. L. Shi, H. K. Huang, F. A. He, K. H. Lam and H. J. Wu, Preparation and characterization of composites based on poly(vinylidene fluoride- co -chlorotrifluoroethylene) and carbon nanofillers: A comparative study of exfoliated graphite nanoplates and multi-walled carbon nanotubes, *J. Mater. Sci.* **54**, 2256 (2019), https://doi:10.1007/s10853-018-3005-x.
[54]H. Ye, L. Yang, W. Z. Shao, S. B. Sun and L. Zhen, Effect of electroactive phase transformation on electron structure and dielectric properties of uniaxial stretching poly (vinylidene fluoride) films, *RSC. Adv.* **3**, 23730 (2013), https://doi:10.1039/c3ra43966f.
[55]C. Tang, B. Li, L. Sun, B. Lively and W. Zhong, The effects of nanofillers, stretching and recrystallization on microstructure, phase transformation and dielectric properties in PVDF nanocomposites, *Eur. Polym. J.* **48**, 1062 (2012), https://doi:10.1016/j.eurpolymj.2012.04.002.
[56]Q. Wang, X. Q. Liu, Z. Qiang, Z. D. Hu, X. Cui, H. X. Wei, J. J. Hu, Y. M. Xia, S. H. Huang, J. M. Zhang, K. Fu and Y. W. Chen, Cellulose nanocrystal enhanced, high dielectric 3D printing composite resin for energy applications, *Compos. Sci. Technol.* **227**, 109601 (2022), https://doi.org/10.1016/j.compscitech.2022.109601.
[57]W. M. Xia, Z. J. Zhou, Y. Liu, Q. Wang and Z. C. Zhang, Crystal phase transition dependence of the energy storage performance of poly (vinylidene fluoride) and poly (vinylidene fluoride-exafluoropropene) copolymers, *J. Appl. Polym. Sci.* **135**, 46306 (2018), https://doi:10.1002/app.46306.